Physicochem. Probl. Miner. Process., 54(2), 2018, 415-427

http://www.journalssystem.com/ppmp

Physicochemical Problems of Mineral Processing

ISSN 1643-1049

Received August 11, 2017; reviewed; accepted September 28, 2017

CO_2 - CH_4 sorption induced swelling of gas shales: An experimental study on the Silurian shales from the Baltic Basin, Poland

Danuta Miedzińska [1], Marcin Lutyński [2]

[1] Military University of Technology, Faculty of Mechanical Engineering, Kaliskiego St. 2, 00-908 Warsaw, Poland
[2] Silesian University of Technology, Faculty of Mining and Geology, Akademicka St. 2, 44-100 Gliwice, Poland

Corresponding author: danuta.miedzinska@wat.edu.pl (Danuta Miedzińska)

Abstract: The main aim of the research presented in the paper was to study the phenomena of shale swelling induced by CH_4 and CO_2 sorption. In the study, a Silurian gas shale sample from the Baltic Basin in Poland was used. Samples represented typical characteristic features of polish shale gas formations with relatively low total organic carbon (0.8%) and high clay mineral content. The first part of the study was devoted to competitive adsorption of CO_2 and CH_4. The second part was devoted to observation of the sorption induced swelling phenomena, where sample linear strains were monitored with the use of strain gauges. Swelling tests were conducted up to the pressure of approximately 8 MPa with CO_2, CH_4 and helium as the baseline. Experimental results were compared with the Seidle and Huitt model where Langmuir constants where determined with volumetric sorption tests. Results of the study showed that matrix swelling in case of CO_2 adsorption was greater than in the case of CH_4 adsorption. The swelling value was directly proportional to adsorption and was about 5 to 10 times smaller than in the case of coal. Sorption of methane and carbon dioxide in the gas-bearing shale was about 10-times lower than in hard coals. The Seidle and Huitt model developed for coals was equally suitable to describe the processes of shale swelling.

Keywords: *shale rock, swelling, methane, carbon dioxide, sorption*

1. Introduction

Despite high natural gas reserves, first shale gas production was started as far as 1821 but resulted in very low efficiencies (Rutter and Keistead, 2012). In the last 30 years, an important progress was made due to the development of drilling technology and the use of horizontal drilling coupled with fracturing stimulation method. The most commonly used method of fracturing is the hydraulic fracturing. This method consists of injecting into the well a large amount of water with proppants and chemical additives in order to crack rocks and to release gas (Tsang and Apps, 2005).

Despite its widespread use, the method mentioned above causes many objections. It can cause groundwater contamination by chemicals used in the fracturing process and requires the use of large amounts of water (EPA, 2016). Consumption and contamination of such significant quantities of water may arise objections in some countries (particularly in the European Union) (Briggs, 2003). A part of water from the hydraulic process returns to the surface as the flowback water, however, it is additionally contaminated with large amounts of dissolved solids, occasionally heavy metals, hence requiring proper utilization methods (EPA, 2016). The described disadvantages of the hydraulic fracturing method resulted in the search for other fracturing media, such as inert gas which is easily condensable and widely available in the environment. One such media is CO_2. A process of injection of CO_2 not only fractures rocks but it can also contribute to the carbon geological storage (Holloway et al., 2006).

Some technologies using non-wetting fluid were presented in (Rogala et al., 2013), involving fracturing with liquid CO_2, nitrogen, LPG and explosive/propellant system - EPS. The current

http://dx.doi.org/10.5277/ppmp1851

fracturing technology is applicable to specific areas with fluid sensitive shale rocks. Based on current hydraulic fracturing performances in Poland, shale has certain volume of low density smectite clay that has tendency to adsorb water based fracturing fluid and to swell (Rogala et al., 2013).

Shale is characterized by its dual porosity system: it contains both primary (micro pores and meso pores) and secondary (macro pores and natural fractures) porosity systems. The primary porosity system contains the vast majority of gas-in-place, while the secondary porosity system provides the conduit for mass transfer to the wellbore. Primary porosity gas storage is dominated by adsorption (Dahaghi, 2010).

Primary porosity is relatively impermeable due to its small pore size. Mass transfer for each gas is dominated by diffusion that is driven by the concentration gradient. A flow through the secondary porosity system is dominated by the Darcy law that relates a flow rate to the permeability and pressure gradient (Dahaghi, 2010).

When the pressure of a natural fracture system in shale drops below the critical desorption pressure, methane starts to desorb from the primary porosity system and is released into the secondary porosity system. As a result, the adsorbed gas concentration in the primary porosity system near the natural fractures is reduced. This reduction in pressure creates a concentration gradient that results in mass transfer by diffusion through the micro and meso porosity (Dahaghi, 2010). The adsorbed gas continues to be released as the pressure is reduced (Cipolla et al., 2009). On the basis of those mechanisms the analyses of the new innovative method of gas shale fracturing and gas recovery coupled with carbon dioxide storage have been developed in the Department of Mechanics and Applied Computer Science of the Military University of Technology in Warsaw, Poland.

Fractured shale reservoir is to some extent similar to a coalbed, where the rock is also source and the sink for the gas. Coal is also characterized by the dual porosity system where gas flows diffusely from coal matrix and then with natural fractures to lower pressure regions (Swami, Settari, 2013).

The characteristic property of gas flow in coal structure is the matrix swelling effect, in which during gas adsorption, coal matrix volume increases, what results in the decrease of coal permeability by decreasing fracture apertures as shown in Fig. 1 (Durucan et al., 2009).

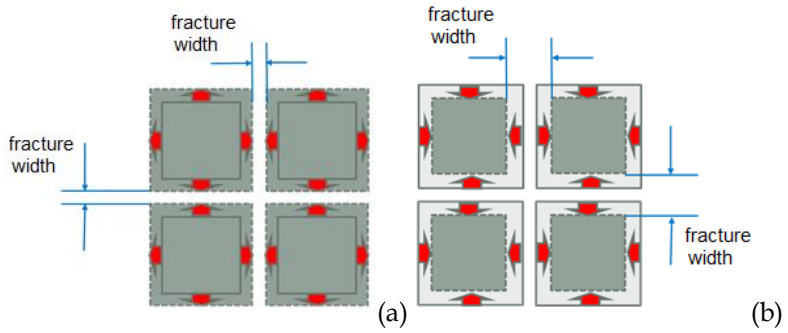

Fig. 1. Rock matrix swelling effect caused by gas adsorption (a) and shrinkage effect caused by gas desorption (b)

During the gas desorption process, a contrary to swelling phenomenon occurs: coal matrix volume decreases, what increases the fracture width and as a result - permeability. Swelling effect can be described with the use of swelling ratio, which for methane sorption on coal is between 2×10^{-4} MPa to 11×10^{-4} MPa and for CO_2 sorption – from 2×10^{-4} MPa to 40×10^{-4} MPa (Joubert et al., 1973; Crosdale et al., 1998; Hildenbrand et al., 2006; Dutta et al., 2006; Day et al., 2008). Previous studies of swelling phenomena on coal show that swelling caused by CO_2 adsorption is approximately twice as much as swelling caused by methane one. This effect has a dramatic impact on the permeability decrease (particularly for low permeability coals < 2 mD) when CO_2 is pumped into the reservoir (Day et al., 2008). In general, swelling of coal is directly proportional to adsorption capacity (Hildenbrand et al., 2006). It is anticipated that similar effect for CO_2 and CH_4 sorption will probably appear in gas bearing shales.

The aim of the research presented in this paper is to study gas exchange effect and swelling phenomenon caused by CO_2 and methane sorption on shale gas rock sample. The samples were

collected from a gas bearing horizon at the depth of 3 km in an exploratory well in Poland. The presented research is a part of developed shale gas recovery Polish technology.

2. Experimental methods and materials

2.1 Sample description

For the purpose of the study Silurian shale rock from the Baltic Basin region with organic carbon content (TOC) of 0.8% was selected. This value of TOC allows to consider rock as a maternal one for hydrocarbons generation. A van Krevelen diagram with marked used sample is shown in Fig. 2. Shale has the gas producing potential (gas generation window), however it can be inconclusive due to the small number of samples used for Rock-Eval analysis. Detailed results of Rock-Eval analysis of the selected samples are presented in Table 1. Quantitative XRD analysis of researched rocks (see Fig. 3) show characteristic features of gas shales from the Baltic-Podlasie-Lublin Basin (Central-Eastern Europe) with relatively low TOC and high clay minerals content (Kuila et al., 2014). Samples designated for the experiments were cut from the cores acquired using core directly from the exploratory well. Only uncracked and visually sound cores were selected for the experiments.

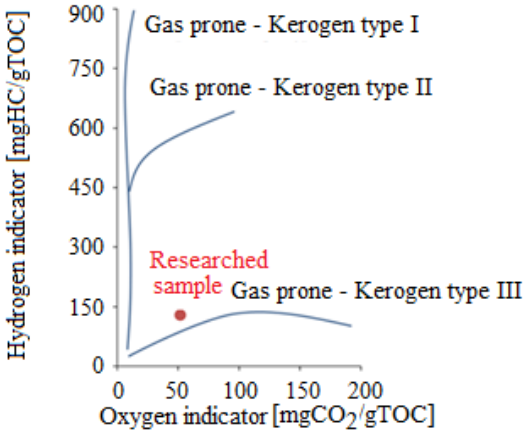

Fig. 2. Van Krevelen diagram showing selected shale sample used for research

Table 1. Results of Rock-Eval analysis of shale rock samples

T_{max} [°C]	S_1 [mgHC/g rock]	S_2 [mgHC/g rock]	S_3 [mgCO_2/g rock]	PI [$S_1/(S_1+S_2)$]	PC [%]
437	0.52	1.04	0.42	0.33	0.15
RC [%]	TOC [%]	HI [mgHC/g TOC]	OI [mgCO_2/gTOC]	total MINC [%]	
0.66	0.81	128	52	1.21	

2.2 Competitive sorption tests

In order to simulate CO_2 pumping and CH_4 recovery process, a typical volumetric sorption setup was used. To measure concentration of outflowing gas the setup was equipped with gas analyzer (Fig. 4). Draeger X-am 7000 gas analyzer was used to measure CH_4 and CO_2 concentration in 0-100% range (accuracy ≤ ±2.0 Vol.% CO_2; ≤ ±5.0 % Vol.% CH_4). Gas pressure and flow on the outlet from the reference cell were regulated by reduction needle valve. The apparatus was placed in a thermostatic bath (stability 0.1°C) to achieve stable temperature of 50°C and consequently to keep CO_2 in supercritical state. Pressure was monitored using WIKA S-20 pressure transducers (accuracy 0.125%) and recorded with APAR205 data acquisition system.

The shale sample was crushed with the use of a mortar to increase its specific surface and to facilitate access to the pores resulting in the acceleration of sorption process. It must be mentioned that

a disk mill was not used for sample preparation since too large disintegration of the sample could result in the changes of primary porosity system.

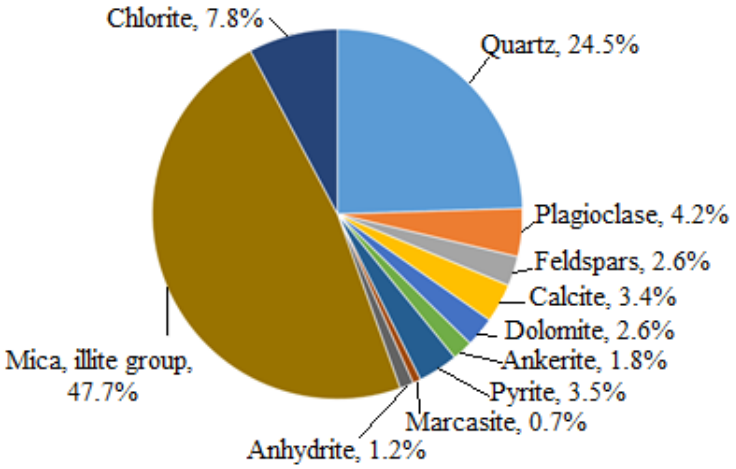

Fig. 3. XRD analysis of shale sample used in tests

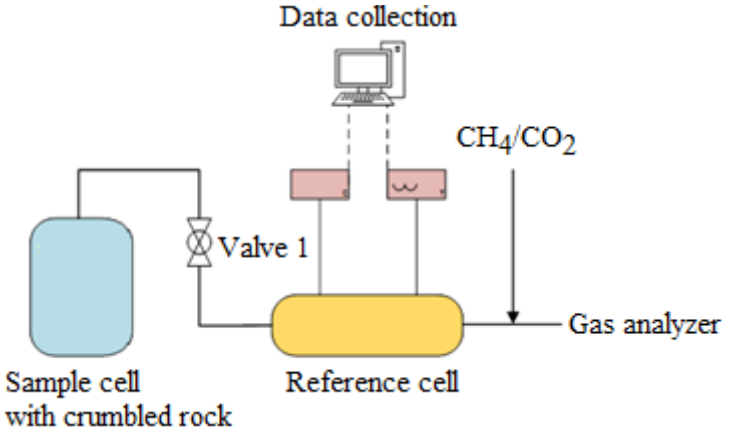

Fig. 4. Scheme of the setup for CO_2/CH_4 competitive sorption tests

The experiment begun after measuring the void volume of the sample cell. For that purpose, a non-sorptive gas (helium) was used. The void volume of the sample cell which consists of apparatus dead volume and pore space was 64.58 cm^3. In the first step of the test the shale rock sample was saturated with methane to the pressure value of 13.71 MPa and sorption equilibrium was achieved after 72 hours. The amount of adsorbed methane was 0.1769 mmol per gram of shale (3.96 m^3 per Mg of dry shale mass). The next steps of the experiment were as follows: methane release from the reference cell with closed valve 1, CO_2 pumping into reference cell to the pressure of 7.3 MPa (supercritical phase), valve 1 opening – gases mixing (24 hours), pressure decrease to 9.07 MPa, valve 1 closing – measurement of gases concentration, gases mixture evacuation from the reference cell, valve 1 opening – desorption and pressure decrease to 6.24 MPa, valve 1 closing – measurement of gases concentration, gases mixture evacuation from the reference cell, valve 1 opening – desorption and consequent pressure decrease to 3.84 MPa, final valve 1 closing – measurement of gases concentration, gases mixture evacuation from the reference cell.

2.3 Swelling measurement method and apparatus

Some research on swelling/shrinkage phenomena of coal matrix can be found in the literature (Reucroft, Sethuraman, 1987; Mazumder, Wolf, 2008; Majewska et al., 2009; Hol et al., 2014; Staib et al., 2014). Swelling/shrinkage measurement methods of this phenomena can be divided into methods using strain gauges, acoustic methods and optical ones.

In the presented study method using strain sensors was applied for rock samples longitudinal elongation measurements. This method was chosen because relatively large pieces of shales were available and there was a possibility to glue strain gauges. Significant advantage of this method is the fact that large samples are more representative for the in-situ conditions. On the other hand, equilibration times are longer and experiments may last up to few months.

The experimental setup (Fig. 5) was designed to measure rock swelling induced by gas adsorption. The apparatus was built of high pressure chamber, 8-channels strain gauges testing system TMX-0108E, pressure transducer and recorder, automatic heating system, data acquisition system, high-pressure pump.

Folic resistance extensometers were glued on the sample surfaces vertically and horizontally to the shale layers with the use of epoxy resin and connected to measurement system. For the purpose of strain measurements in comparison to the initial state it was decided to place the referenced samples outside the high-pressure chamber.

Wires soldered to the strain gauges were led out from the high-pressure chamber (Fig. 5) via the SWAGELOK through-connector system additionally filled with glue. Pressure was measured using a pressure sensor WIKA while the temperature using Pt100 sensor (1/3 class B). Pressure of supplied gas was increased by the pump MAXIMATOR DLE-15-30. Pressure and temperature readings were recorded with APAR205 recorder while strain values using an eight-channel strain gauge measurement system - TENMEX TMX-0108. The high-pressure chamber was wrapped with heating tape and placed in an isolated chamber in order to simulate in-situ temperature conditions.

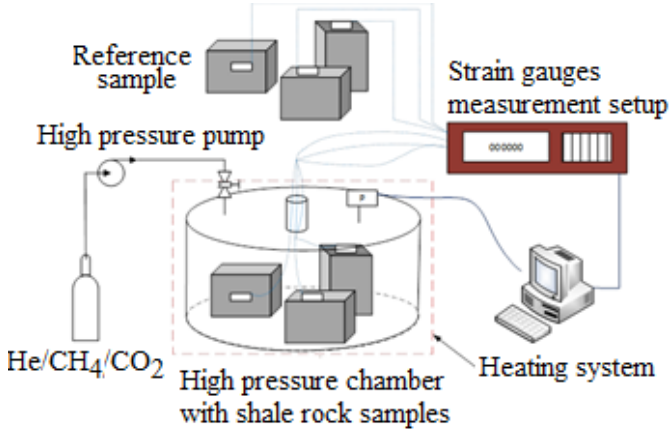

Fig. 5. Scheme of setup for gas shale swelling/shrinkage measurements

The apparatus contained four samples with two strain gauges for each one glued parallel and perpendicularly to the lamination (Fig. 6). Samples (marked as S1, S2, S3) were cut out from the drilling core and additionally divided into four equal quadrants cut along their diameter. The samples were approximately 2 cm thick and had approximated dimensions of 3x3x3.5 cm.

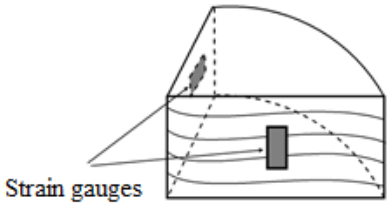

Fig. 6. Strain gauges location on shale sample

After placing the samples in a high-pressure chamber and removal of the leakage in strain gauge section there was a circuit disruption causing measurement problems for some of the samples. Finally, the successful full range measurements were performed for two samples (vertical and horizontal strain). Because of the lack of tested material, the standard error was not considered.

Due to the limitations associated with the setup the tests were conducted up to the pressure of 8 MPa. Prior to the measurement, the measuring system was reset and the injection of the gas was performed in increments of 1.5 MPa being the compromise between long equilibration time and pressure increments commonly used in sorption measurements.

After completion of the inert gas experiments similar tests were continued on the same samples using methane and carbon dioxide respectively. Between the tests, samples were gradually degassed to atmospheric pressure, and then subjected to a vacuum for a period of several days in order to remove residual gas. The process of sample degassing was terminated when the strain gauges readings were coming back to approximately initial values (Fig 7a). Gas at each incremental step was injected after the sorption equilibrium was observed, e.g. gauge readings were stable what usually lasted several days (Fig. 7b).

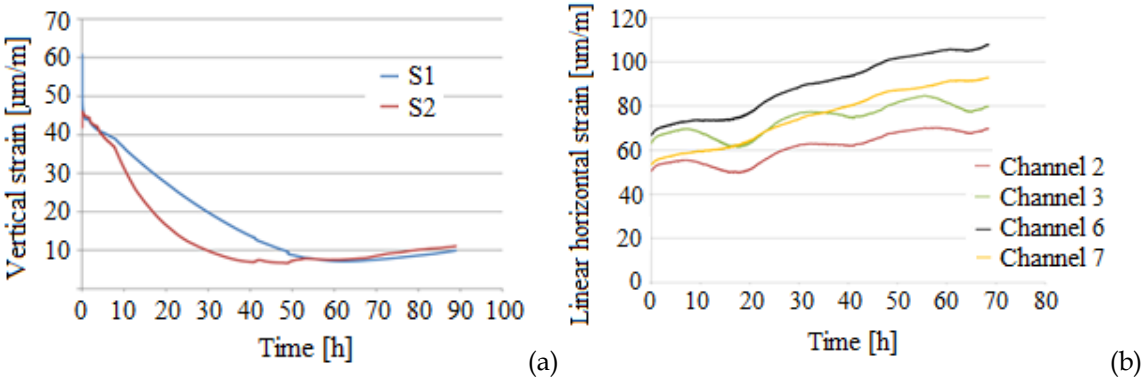

Fig. 7. (a) Example of gradual desorption of gas (from approx. 3 MPa) and shale shrinkage for two samples S1 and S2 (b) Example of recorded linear horizontal strain of samples for methane adsorption under 6 MPa pressure

3. Results and discussion

3.1 Competitive sorption tests

From the pumped gases mass balance calculations, it can be concluded that the amount of methane in the setup after sorption was 393.17 mmol, in which 376.19 mmol was a free gas (not adsorbed) and 16.98 mmol adsorbed on the sample, which gives 0.1769 mmol/g of gas adsorbed (per mass of solid). In total, 628.9 mmol of CO_2 (marked as $n_{CO_2}^{total}$) was injected into the setup. It gives the initial concentration of CH_4/CO_2 in the mixture of 37.43%vol./62.57%vol. respectively - considering there is no adsorption. It means that increase in methane concentration in each step of desorption process is caused by preferential adsorption of CO_2 since the concentration of gases was measured in each desorption step. The results of measurements are shown in Fig. 8.

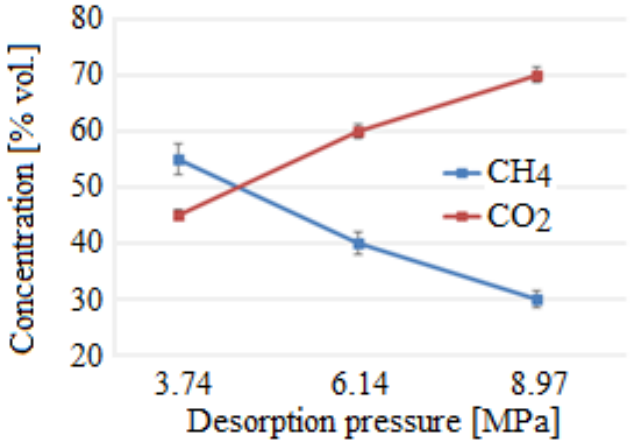

Fig. 8. Results of competitive sorption test for shale rock sample as CO_2/CH_4 concentration vs. desorption pressure chart

Considering that it is difficult to precisely describe the amount of adsorbed gas on the base of its concentration in free phase, it was assumed that:

$$n_{CO_2}^{free} = \frac{n_{CH_4}}{p_{CH_4}^{av}} - n_{CH_4} \quad (1)$$

where: $n_{CO_2}^{free}$ is the calculated amount of free CO_2 [mol], $p_{CH_4}^{av}$ is the average partial pressure of CH_4, n_{CH_4} is the total amount of CH_4 [mol]. Approximation of adsorbed CO_2 can be calculated on the assumption that:

$$n_{CO_2}^{sorb} = n_{CO_2}^{total} - n_{CO_2}^{free}. \quad (2)$$

On the base of Eq. (2) the amount of adsorbed CO_2 in the experiment was 78.47 mmol (0.817 mmol per gram of shale sample). This amount is 4.5 times higher than the amount of adsorbed methane. Experiments described in Section 3.5 proved this observation although the ratio of CO_2:CH_4 sorption is slightly lower.

Presented results show that alike in other organic sorbents preferential adsorption of CO_2 to CH_4 in shale samples appeared, even for quite low pressure values. Hence, one can assume that the effect of enhanced desorption of CH_4 appeared.

3.2 Swelling tests - determination of mechanical compliance factor

The first stage of the swelling experiment was devoted to the determination of deformations that occur during submission of shale samples to inert gases. As a consequence, the calculation of the mechanical compliance factor (C_p) was carried out. For this purpose, a first set of swelling tests was performed with helium.

Determination of the mechanical compliance factor (C_p) was performed to define strain of the sample exposed to the external gas pressure. In experimental swelling tests, sorption deformation and induced impact of the gas on the sample external surface cancel each other out (Fig. 9). Therefore, the measured swelling of the sample is called the "net" deformation. It can be assumed that the deformation of the sample (ε_r) is directly proportional to gas pressure:

$$\varepsilon_r = -C_p P \quad (3)$$

where C_p is the mechanical compliance factor [MPa^{-1}].

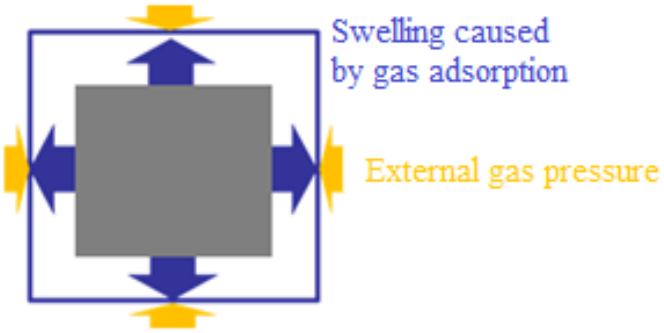

Fig. 9. Diagram of forces impacting rock sample during gas adsorption and related strains

Observation of the deformation caused by sorption of helium in coals showed that strain should be negative causing the sample to shrink because gas is not adsorbed and does not contribute to the swelling effect. In these experiments, similar observations were recorded. Apparently, shale matrix shrunk under the pressure of inert gas. Linear strain with matching trend lines used for calculations of C_p factor is shown in Fig. 10.

Linear strains of shale samples with calculated mechanical compliance factors (C_p) are shown in Table 2. From Table 2 it is clear that the coefficients (factors) of mechanical compliance have similar values for horizontal and vertical deformations (strains) for both samples. In each sample values of C_p for vertical deformations are higher. This might be explained by the typical features of shales –

lamination and cleavage. Different strains of the sample are the result of anisotropy of samples which is often visible in uniaxial strength tests (Shovkun and Espinoza, 2017; Yan et al., 2017).

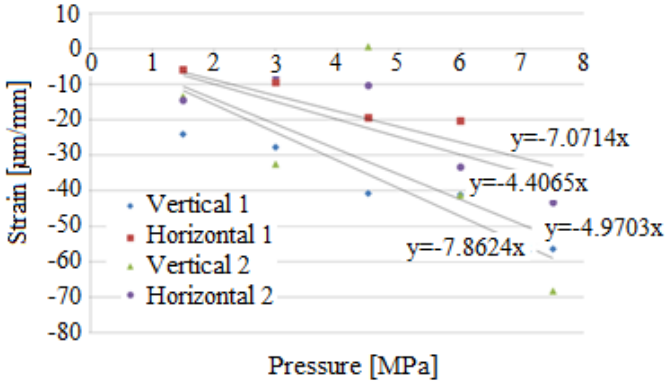

Fig. 10. Test results for linear strain for two shale samples in function of helium pressure

Table 2. Test results for linear strain of shale samples with calculated mechanical compliance factors (C_p)

Pressure [MPa]	Strain [μm/m]			
	Vertical 1	Horizontal 1	Vertical 2	Horizontal 2
1.5	-24.06	-5.92	-13.47	-14.48
3.0	-27.72	-9.48	-32.56	-7.50
4.5	-40.76	-19.47	0.60	-10.26
6.0	-41.16	-20.23	-41.27	-33.33
7.5	-56.45	-39.86	-68.30	-43.29
C_p	-0.786	-0.4407	-0.707	-0.497

3.3 CH_4 and CO_2 adsorption induced swelling

Linear strain recording ε_m is carried out in [μm/m] for two surfaces, however sample volumetric strain is more representative and can be defined as the sum of vertical deformation and horizontal deformation multiplied by two. This assumption is commonly used in rock mechanics (Wang, 2016):

$$\frac{\Delta V}{V} = \varepsilon_{vertical} + 2 \cdot \varepsilon_{horizontal} \,. \tag{4}$$

Methane adsorption induced volumetric strain is shown in Fig.11, while volumetric strain of shale exposed to carbon dioxide adsorption – in Fig. 12.

Results presented in Figs. 11 and 12 show that volumetric strain in case of CO_2 sorption is greater than in case of methane one. The size of volumetric deformations, similarly to gas adsorption, is about 10-times lower than in case of coals. Results were compared with the results obtained in (Battistutta, 2010) for anthracite Selar Cornish coal from the UK (Fig. 13).

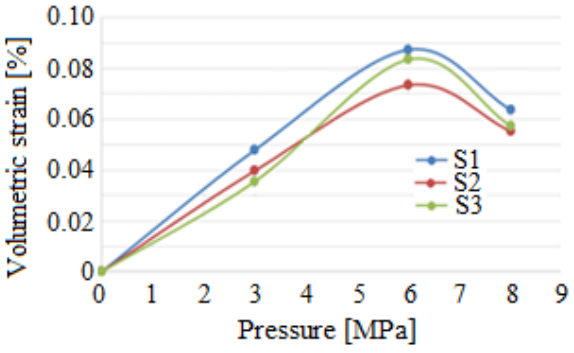

Fig. 11. Test results for volumetric strain of shale samples (S1, S2, S3) exposed to CH_4 at 30°C

It should be noted that coal sample used for comparison is a high-rank coal and results of Durucan et al. (2008) indicate that high rank coals have noticeably greater swelling effect, which as mentioned before, is directly proportional to the sorption capacity. For low rank coals, swelling factor a is usually lower. The comparison of these coefficients using data obtained for shale and coal is presented in the next section.

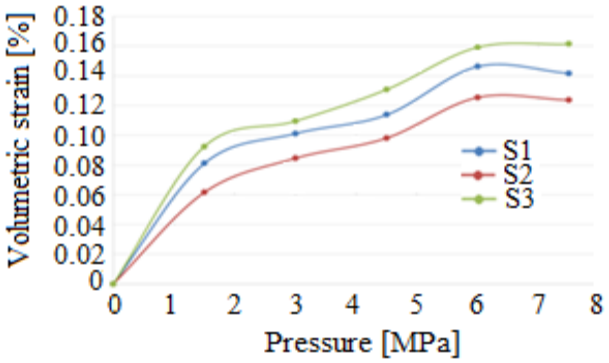

Fig. 12. Test results for volumetric strain of shale samples (S1, S2, S3) exposed to CO_2 at 30°C

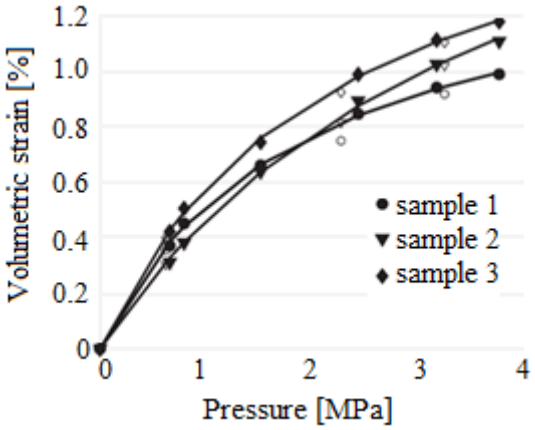

Fig. 13. Results of coal matrix swelling/shrinkage during sorption of CO_2 on Selar Cornish coal samples (adsorption - filled points; desorption - points without the filling) (after Battistutta et al., 2010)

3.4 Application of the Seidle and Huitt model

Results of swelling tests show that the volumetric strain curve (Fig. 11 and 12) are similar to the type I sorption isotherm, so it can be assumed that the deformation (strain) is directly proportional to the sorption. These results are consistent with the observations made in similar studies for hard coals (Durucan et al., 2008; Battistutta et al., 2010, Hol et al., 2014; Seidle and Huitt, 1995)

In order to verify that assumption the Seidle and Huitt model (Hol et al., 2014) was applied since it relates Langmuir isotherm to the strain of the sample:

$$\varepsilon_m = \alpha \cdot V_L \cdot \frac{P}{P_L+P} \tag{5}$$

where ε_m is strain (0 at atmospheric pressure), a - matrix swelling coefficient [kg/m^3], P -pressure [MPa], and P_L and V_L - Langmuir isotherm constants. In addition to the swelling the sample should experience the deformation (compression) caused by gas pressure acting on the external surface of the sample (mentioned earlier).

Therefore, the measurement study of swelling is the "net" deformation as follows:

$$\varepsilon_{exp} = \varepsilon_m - c_p \cdot P \tag{6}$$

or

$$\varepsilon_m = \varepsilon_{exp} + c_p \cdot P = \alpha \cdot V_L \frac{P}{P_L+P} \tag{7}$$

in this case C_p coefficient must be determined experimentally (see Section 3.2).

3.5 Determination of sorption isotherms

The use of the model describing matrix swelling caused by gas sorption requires calculations of the Langmuir model constants (V_L and P_L). In order to do this, experimental determination of the adsorption isotherm for each gas is required.

The basic model of Langmuir isotherm has the following form (Zheng et al., 2009):

$$V = \frac{V_L \cdot P}{P_L + P} \tag{8}$$

where V - moles of gas adsorbed per mass of sorbent [mmol/g], V_L – Langmuir volume (e.g. maximum sorption capacity) [mmol/g], P_L – Langmuir pressure [MPa], P – pressure [MPa].

The isotherm was determined using the manometric setup described in Section 2.2. In order to calculate the excess sorption in each step, the following formula is used:

$$m^{CO_2} = \sum_{i=1}^{N} V_{ref} \cdot \left(\rho_i^{f,CO_2} - \rho_i^{e,CO_2}\right) \tag{9}$$

where V_{ref} is the reference cell volume [cm^3] while ρ with superscripts f, CO_2 and e, CO_2 are gas densities during the stage of reference volume filling (before opening the Valve 1 connecting reference volume with the sample cell) and sorption equilibrium phase (when the Valve 1 is open). It is important that the used equation of gas state is sufficiently accurate to properly describe its behavior in supercritical conditions (e.g. above the pressure of 7.39 MPa and a temperature of 31.1° C for CO_2), since it significantly affects the accuracy of the results. Such conditions occur in unconventional gas reservoirs such as gas-bearing shales or deep coal seams. Therefore, the accurate Span and Wagner equation of state for CO_2 (Span and Wagner, 1995), McCarthy for helium (McCarthy and Arp, 1990) and Wagner and Span (Wagner and Span, 1993) for methane is used.

CH_4 and CO_2 sorption isotherms on shales are presented in Fig. 14 and 15. It should be noted that obtained results confirmed those from experiments of the CH_4-CO_2 gas exchange. The maximum excess CO2 adsorption is about 2.5-3 times higher than in case of CH_4.

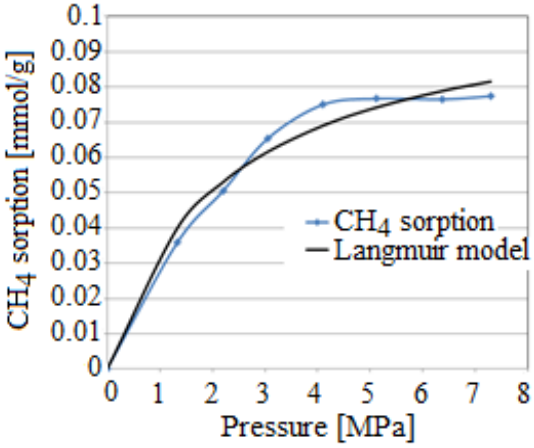

Fig. 14. Methane sorption isotherms for shale samples at 50 °C

Slight deviation of sorption results for CO_2 in the region of pressure over 3 MPa is caused by the method error. Gas in the reference cell is in the supercritical phase, it is a phase very sensitive to the thermodynamic changes and keeping it in a stable condition was very difficult. Overall, calculated Langmuir constants match the data found in literature (Khrosrokhavar et al., 2014). Langmuir model constants determined for the analyzed samples are shown in Table 4.

Table 4. Langmuir model constants determined for the analyzed shale samples

	V_L [mmol/g]	P_L [MPa]
CH_4	0.10	4.43
CO_2	0.25	1.05

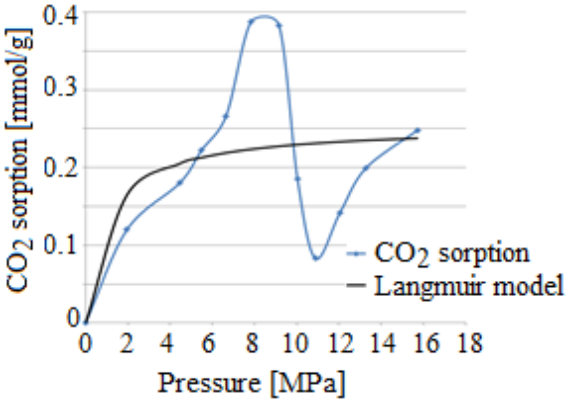

Fig. 15. CO_2 sorption isotherm for shale sample at 50 °C

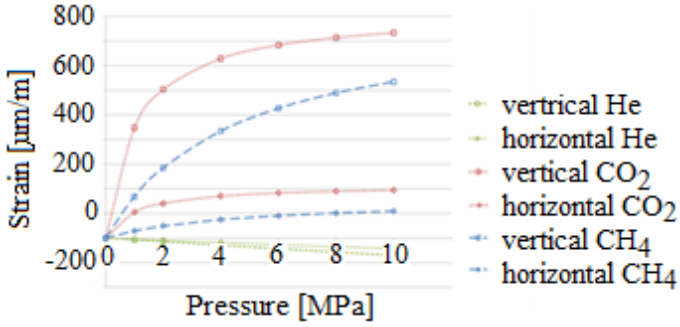

Fig. 16. Test results for linear strain curves of shale sample

On the base of the determined Langmuir model constants, C_p coefficient and the matrix swelling factor α, linear strain curves for each gas were determined (Fig. 16).

Additionally, linear strain was recalculated to volumetric strain and prediction of volumetric strains for the pressure of 30-35 MPa (reservoir pressure of gas bearing shale horizons in Poland) was made. The forecast presented on the background of experimental points is shown in Fig. 17.

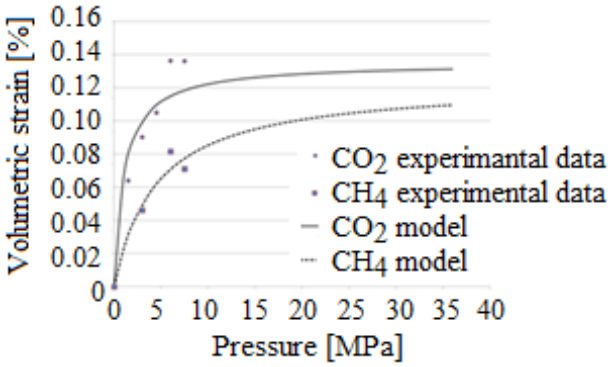

Fig. 17. Comparison of volumetric strains of swelling shale sample modeled with Seidle and Huitt model with experimental data

Calculated shale gas matrix swelling factors were compared with the coefficients of coal swelling presented in Battistutta (2010) and the Langmuir constant V_L in Table 5.

A comparison of obtained results with data for hard coal indicates that the matrix swelling coefficients presented similar values but the swelling of shale sample is much lower because of the lower sorption capacity. An interesting observation is that the shale gas matrix swelling coefficient α for CH_4 is greater than that for CO_2. This is the opposite phenomenon than that observed for coals.

However, very low values of Langmuir constant V_L for CH_4 caused that the swelling of the shale sample was proportionally lower than for CO_2 adsorption.

Table 5. Comparison of swelling coefficient α and Langmuir constant V_L for shale and coals (Durucan et al. 2008)

	Flame coal	Anthracite	Silurian shale
Coefficient of matrix swelling (CH_4) a, [kg/m^3]	0.15-0.4	0.48-0.82	0.52
Coefficient of matrix swelling (CO_2) a, [kg/m^3]	0.3-0.8	0.5-1.6	0.24
Langmuir constant V_L (average value), [dm^3/kg]	6-14	16-25	2.4-6.1

4. Summary

The research led to the development of the full methodology of the swelling sorption measurements of gas bearing shales induced by adsorption process. So far, such studies were conducted only on hard coals. The processes of rock swelling are particularly important in case of low-permeable rock formations, where additional processes of physical sorption may increase volume of the rock matrix and as a consequence reduce permeability by closing the fracture aperture.

Finally, it can be concluded that for tested shale rocks the matrix swelling in case of CO_2 adsorption is greater than in case of CH_4 adsorption. Next, the swelling value is directly proportional to the adsorption and is about 5 to 10 times smaller than in case of coal. The calculated matrix swelling factors α are approximately 0.2-0.5 kg/m^3, where in case of coals those values are in the range of 0.2-1.6 kg/m^3. Sorption of methane and carbon dioxide in the gas-bearing shale is about 10-times lower than in hard coals.

One of key findings of the study is that the Seidle and Huitt Model is suitable to describe the processes of shale swelling.

The presented research is a part of a development of the technology of a shale gas recovery with the use of CO_2. Achieved results can have an impact on the gas recovery with the use of CO_2 when comparing to water-based fracturing methods.

Acknowledgements

The paper is supported by grant No BG2/DIOX4SHELL/14 titled "Development of guidelines for design of innovative technology of shale gas recovery with the use of liquid CO_2 on the base of numerical and experimental research –DIOX4SHELL", supported by the National Centre for Research and Development (NCBR) in years 2014-2017.

References

TSANG, C.-F., APPS, J.A., 2005, *Underground Injection Science and Technology*, Elsevier B.V.

BATTISTUTTA, E., VAN HEMERT, P., LUTYNSKI, M., BRUINING, H., WOLF, K.-H., 2010. *Swelling and sorption experiments on methane, nitrogen and carbon dioxide on dry Selar Cornish coal*. Int. J. Coal Geol., 84, 39-48.

BRIGGS, D., 2003. *Environmental pollution and the global burden of disease*. British Medical Bulletin, 68, 1-24.

CIPOLLA, C.L., LOLON, E.P., ERDLE, J.C., RUBIN, B., 2009. *Reservoir modeling in shale gas reservoirs*. SPE125530, Charleston, West Virginia.

CROSDALE, P.J., BEAMISH, B.B., VALIX, M., 1998. *Coalbed methane sorption related to coal composition*. Int. J. Coal Geol., 35, 147-158.

DAHAGHI, K.A., 2010. *Numerical Simulations and Modeling of Enhanced Gas Recovery and CO_2 Sequestration in Shale Gas Reservoir*s. SPE, West Virginia University.

DAY, S., DUFFY, G., SAKUROVS, R., WEIR S., 2008. *Effect of coal properties on CO_2 sorption capacity under supercritical conditions*. Int. J. Greenhouse Gas Control, 2, 342-352.

DURUCAN, S., AHSANB, M., SHIA, J.-Q., 2008. *Matrix shrinkage and swelling characteristics of European coals*. Energy Proc., 3055-3062.

DUTTA, P., HARPALANI, S., PRUSTY, B., 2008. *Modeling of CO_2 sorption on coal*. Fuel, 87, 2023-2036.

EPA, 2016. *Study of Hydraulic Fracturing and Its Potential Impact on Drinking Water Resources*. www.epa.gov.pl.

HILDENBRAND, A., KROOSS, B.M., BUSCH, A., GASCHNITZ, R., 2006. *Evolution of methane sorption capacity of coal seams as a function of burial history – a case study from the Campine Basin, NE Belgium*. Int. J. Coal Geol., 66, 179-203.

HOL, S., GENSTERBLUM, Y., MASSAROTTO, P., 2014. *Sorption and changes in bulk modulus of coal - experimental evidence and governing mechanisms for CBM and ECBM applications*. Int J. Coal Geol., 128-129, 119-133.

HOLLOWAY, S., KARIMJEE, A., AKAI, M., PIPATTI, R., RYPDAL., K., 2006. *Carbon Dioxide Transport, Injection and Geological Storage*. IPCC Guidelines for National Greenhouse Gas Inventories.

JOUBERT, J.I., GREIN, C.T., BIENSTOCK, D., 1973. *Sorption of methane in moist coal*. Fuel, 52, 181-185.

KHOSROKHAVAR, R., WOLF, K.-H., BRUINING, H., 2014. *Sorption of CH_4 and CO_2 on a carboniferous shale from Belgium using a manometric setup*. Int. J. Coal Geol., 128-129, 153-161.

KUILA, U., MCCARTY, D.K., DERKOWSKI, A., FISCHER, T.B., TOPÓR, T., PRASAD, M., 2014. *Nano-scale texture and porosity of organic matter and clay minerals in organic-rich mudrocks*. Fuel, 135, 359-373.

MAJEWSKA, Z., CEGLARSKA-STEFAŃSKA, G., MAJEWSKI, S., ZIETEK, J., 2009. *Binary gas sorption/desorption experiments on a bituminous coal: Simultaneous measurements on sorption kinetics, volumetric strain and acoustic emission*. Int. J. of Coal Geol., 77, 90-102.

MAZUMDER, S., WOLF, K.H., 2008. *Differential swelling and permeability change of coal in response to CO_2 injection for ECBM*. SPE Asia Pacific Oil and Gas Conference and Exhibition "Gas Now: Delivering on Expectations", 267-298.

MCCARTY, R.D., ARP, V.D., 1990. *A New Wide Range Equation of State for Helium*. Adv. Cryogen. Eng., 35, 1465-1475.

REUCROFT, P.J., SETHURAMAN, A.R., 1987. *Effect of pressure on carbon dioxide induced coal swelling*. Energy Fuels, 1, 72-75.

ROGALA, A., KRZYSIEK, J., BERNACIAK, M., HUPKA, J., 2013. *Non-Aqueous Fracturing Technologies for Shale Gas Recovery*. Physicochem. Probl. Miner. Process., 49, 313-322.

RUTTER, P., KEIRSTEAD, J., 2012. *A brief history and the possible future of urban energy systems*. Energy Policy, 50, 72-80.

SEIDLE, J.P., HUITT, L.G., 1995. *Experimental Measurement of Coal Matrix Shrinkage due to Gas Desorption and Implications for Cleat Matrix Increases*. SPE Paper 30010.

SHOVKUN, I., ESPINOZA, D.N., 2017. *Coupled fluid flow-geomechanics simulation in stress-sensitive coal and shale reservoirs: Impact of desorption-induced stresses, shear failure, and fines migration*. Fuel, 195, 260–272.

SPAN, R., WAGNER, W., 1995. *A New Equation of State for Carbon Dioxide Covering the Fluid Region from the Triple-point Temperature to 1100 K at Pressures up to 800 MPa*. J. Phys. Chem. Ref. Data, 25, 1509-1596.

STAIB, G., SAKUROVS, R., GRAY, E.M., 2014. *Kinetics of coal swelling in gases: Influence of gas pressure, gas type and coal type*. Int. J. Coal Geol., 132, 117-122.

SWAMI, V., SETTARI, A., 2013. *A Numerical Model for Multi-mechanism flow in Shale Gas Reservoirs with Application to Laboratory Scale Testing*. SPE Paper 164840.

WAGNER, W., SPAN, R., 1993. *Special Equations of State for Methane, Argon, and Nitrogen for the Temperature Range from 270 to 350 K at Pressures up to 30 MPa*. Int. J. Thermophys., 14, 699-725.

WANG, H.F., 2016. *Theory of Linear Poroelasticity with Applications to Geomechanics and Hydrogeology*. Princeton University Press.

WANG, K., WANG, G., REN, T., CHENG, Y., 2014. *Methane and CO_2 sorption hysteresis on coal: A critical review*. Int. J. Coal Geol., 132, 60-80.

YAN, C., DENG, J., CHENG, Y., LI, M., FENG, Y., LI, X., 2017. *Mechanical Properties of Gas Shale During Drilling Operations*. Rock Mech. Rock Eng., 50, 1-13.

ZHENG, H., LIUA, D., ZHENGA, Y, LIANG, S., LIUA, Y., 2009. *Sorption isotherm and kinetic modeling of aniline on Cr-bentonite*. J. Hazard. Mater., 167, 141-147.